Investigation of microstructure changes in ODS-EUROFER after hydrogen loading

O.V. Emelyanova [a, *], M.G. Ganchenkova [a, b], E. Malitskii [b], Y.N. Yagodzinskyy [b], M. Klimenkov [c], V.A. Borodin [a, d], P.V. Vladimirov [c], R. Lindau [c], A. Möslang [c], H. Hänninen [b]

[a] National Research Nuclear University MEPhI (Moscow Engineering Physics Institute), Kashirskoe Sh. 31, 115409 Moscow, Russia
[b] Aalto University, School of Engineering, FI-00076 Aalto, Finland
[c] Karlsruhe Institute of Technology, Institute for Applied Materials Applied Materials Physics, Hermann-von-Helmholtz-Platz 1, 76344 Eggenstein-Leopoldshafen, Germany
[d] National Research Centre "Kurchatov Institute", Kurchatov Sq. 1, 123182 Moscow, Russia

ARTICLE INFO

Keywords:
Hydrogen
ODS steel
Thermal desorption spectroscopy
HRTEM
Ab initio
Molecular dynamics

ABSTRACT

The effect of hydrogen on the microstructure of mechanically tested ODS EUROFER steel was investi gated by means of transmission electron microscopy, thermal desorption spectroscopy, and atomistic simulations. The presence of yttrium oxide particles notably increases hydrogen uptake in ODS EUROFER steel as compared to ODS free EUROFER 97. Under tensile loading, hydrogen accumulation promotes the loss of cohesion at the oxide particle interfaces. First principles molecular dynamics simulations indicate that hydrogen can be trapped at nanoparticle/matrix interface, creating OH groups. The accumulation of hydrogen atoms at the oxide particle surface can be the reason for the observed hydrogen induced oxide/matrix interface weakening and de cohesion under the action of external tensile stress.

1. Introduction

The reduced activation ferritic martensitic (RAFM) oxide dispersion strengthened (ODS) steels have a great potential to be employed as high performance structural materials for fusion re actors, advanced fission reactors, as well as accelerator driven system (ADS) devises [1,2].

The materials usage in severe radiation environments implies that, in addition to the improved mechanical stability, they must be resistant to the deleterious effects of radiation. The ODS steels as compared to conventional ones allow an increase of the operation temperature up to 650 °C due to their enhanced resistance to high temperature creep [3]. It is also suggested that high concentration of nanoparticles further improves swelling resistance because the oxide particles may serve as efficient traps for helium, preventing its accumulation at grain boundaries [4–6]. However, the operation conditions of the advanced fission and future fusion facilities will be much more severe than in the modern nuclear reactors. In particular, hydrogen production rates are predicted to be 41 appm/dpa in fusion applications, 30–300 appm/dpa in spallation source (ESS), and only 0.7 appm/dpa in fast breeder reactor (BOR 60) [7]. In such conditions, it is not obvious whether the beneficial effects of nanoparticle strengthening on mechanical properties, such as high temperature creep resistance, will not be overcome under irradia tion by other degradation mechanisms. For instance, recent in vestigations [8,9] have demonstrated that hydrogen accumulation in ODS steels brings a risk of mechanical property degradation such as hydrogen embrittlement (HE) and stimulates swelling when accompanied with helium [10]. Despite potential risks for ODS steel performance from dissolved hydrogen isotopes, the mechanisms of hydrogen interaction with oxide particles are far from being fully clarified. Of particular interest is the effect of hydrogen on the properties of oxide/matrix interface. This work addresses this issue by means of a combination of experimental (transmission electron microscopy and thermal desorption spectroscopy) and atomistic simulation techniques. It is demonstrated, in particular, that

* Corresponding author.
E-mail address: eolga@bk.ru (O.V. Emelyanova).

hydrogen accumulation at the interface leads under tensile loading to nanoparticle de cohesion from the matrix, which can trigger off microcrack nucleation at oxide particle/matrix interface under the action of external loading.

2. Experimental and simulation methods

Reduced activation ferritic martensitic (RAFM) steel ODS EUROFER was fabricated by mechanical alloying of inert gas atomised steel EUROFER 97 (9% CrWVTa) together with 0.3 wt% of yttria powder and consolidating the mixture using hot isostatic pressing (HIP). The resultant elemental composition of ODS EUROFER steel is similar to that of EUROFER 97 steel [3]. A detailed description of the fabrication process is presented else where [3]. Sub sized tensile specimens with the size of about $0.2 \times 4 \times 9$ mm were cut from both ODS EUROFER and ODS free EUROFER 97 steels using a spark erosion machine parallel to the rolling direction of the material billet.

Hydrogen was introduced electrochemically from 0.1N NaOH solution with 20 mg/l of $CS(NH_2)_2$. Hydrogen charging was per formed at controlled electrochemical potential of -1.85 V_{Hg/Hg_2SO_4} for 24 h. The hydrogen uptake was measured using the thermal desorption spectroscopy (TDS) apparatus in the temperature range from RT to 850 °C under controlled heating rate of 6 °C/min. The specimens for TDS measurements were cut from the gauge length of the tensile specimens after their hydrogen charging and testing.

The constant extension rate tensile (CERT) tests were performed with 2 kN Deben loading device at strain rate of 10^{-4} s^{-1}. Speci mens were tested in air in as supplied state and after electro chemical pre charging with hydrogen. Tensile tests of the hydrogen charged specimens were performed immediately after electrochemical pre charging.

The microstructure of as supplied and hydrogen charged ODS EUROFER samples was studied after mechanical testing using a FEI Tecnai 20 F microscope (200 kV, field emission gun) equipped with a high angle annular dark field (HAADF) detector. The energy dispersed X ray spectroscopy (EDX) measurements were per formed in the scanning transmission electron microscopy (STEM) mode. Cross section samples for transmission electron microscopy (TEM) examinations were cut with a focused ion beam (FIB) lift out technique along the tensile load axis at the distance of 300 μm from the fracture surface and 5–8 μm from the outer surface.

The kinetics of atomic hydrogen at the interface between the iron matrix and yttrium oxide nanoparticle was studied in the framework of the density functional theory (DFT) approach implemented in plane wave based code VASP [11]. The calcula tions used the generalized gradient approximation (GGA) with Perdew–Burke–Ernzerhof exchange correlation functional [12]. The cubic simulation supercell was constructed based on body centered cubic (bcc) iron lattice containing $6 \times 6 \times 6$ elementary cells (432 lattice sites), where 36 atoms in a cubic volume were eliminated and the free space was filled with 14 yttrium atoms and 6 oxygen atoms arranged as in an ideal crystal of Y_2O_3. The crystal was arbitrary selected as Y terminated. Though subsequent simulations indicated that an alternative choice (O termination) might be a better one, it is not critical for the current study, which is aimed at the investigation of hydrogen behavior. Prior to H insertion, the simulation cell was statically relaxed and then a H atom was added near the particle interface. The subsequent dy namics of the H atom was studied using the first principles mo lecular dynamics (MD) approach, as implemented in VASP. Having in mind the high mobility of hydrogen, the time step was selected equal to only 0.5 fs and the whole run took ~140 fs. The temper ature was maintained at the level of 1000 K using the Nosé Hoover thermostat.

3. Results and discussion

3.1. TDS measurements

Typical TDS curves after hydrogen pre charging and tensile testing for ODS EUROFER and EUROFER 97 steels are shown in Fig. 1. The TDS curves of both investigated steels demonstrate single release peak located at 415 K which is typical for bcc metals [13–15]. However, ODS EUROFER steel shows markedly higher hydrogen uptake as compared to that of EUROFER 97 steel. The hydrogen content in the specimens was estimated by integration of obtained TDS curves. The total hydrogen concentrations were found to be 93 appm and 19 appm for ODS EUROFER steel and EUROFER 97 steel, respectively, in agreement with [9,16]. This can be a reflection of ODS Eurofer specific microstructural features, such as enhanced total area of grain boundaries and dislocation density. In addition, a significant amount of hydrogen can be trapped at ODS particle/matrix interfaces. To shed light on impor tance of yttrium oxide particles as H trapping centers, micro structural analysis and first principles MD simulations have been performed.

3.2. Microstructure investigations

In order to reveal the role of yttrium oxide particles in the process of hydrogen accumulation in ODS EUROFER steel, TEM examinations were performed. As shown in Fig. 2, the sample in as supplied state has a typical microstructure of ODS EUROFER steel [3,9]. The grains with a mean size of about 0.6–1 μm are elongated in the rolling direction. Yttrium oxide nanoparticles have the mean size of about 10–15 nm, the number density is about 1.2×10^{22} m^{-3}, and they are distributed uniformly over the grains.

According to Ref. [17], the microstructure of the undistorted ODS particles (Fig. 2b) in the ODS EUROFER steel can be described as a core–shell structure. The EDX analysis across the particle matrix interface shows that the reduction of matrix element content (iron and chromium) occurs simultaneously with the increase of ODS elements (yttrium and oxygen) without a noticeable gap. In addition, a certain increase of Cr concentration above the matrix average is detected close to the nanoparticle/matrix interface forming a Cr rich shell. For more details on core–shell structure of oxide particles in ODS EUROFER steel see Fig. 3 in Ref. [17].

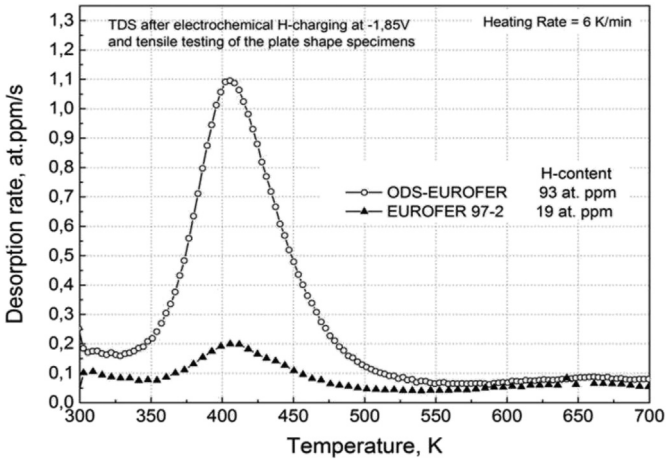

Fig. 1. TDS curves of ODS-EUROFER and EUROFER 97 steels after hydrogen charging for 24 h and following tensile testing.

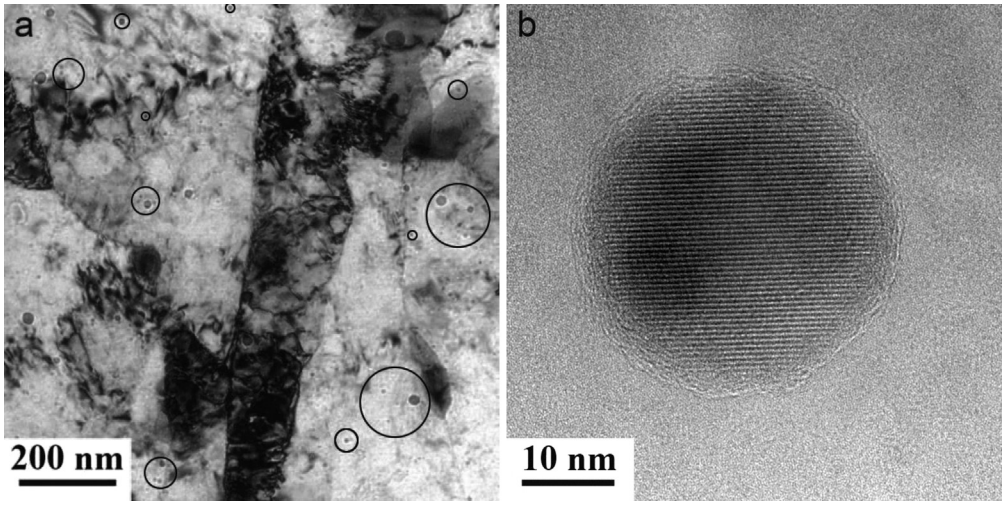

Fig. 2. TEM micrographs of ODS-EUROFER steel in as-supplied state after CERT tensile testing: (a) general view; (b) HRTEM image of an yttrium oxide particle.

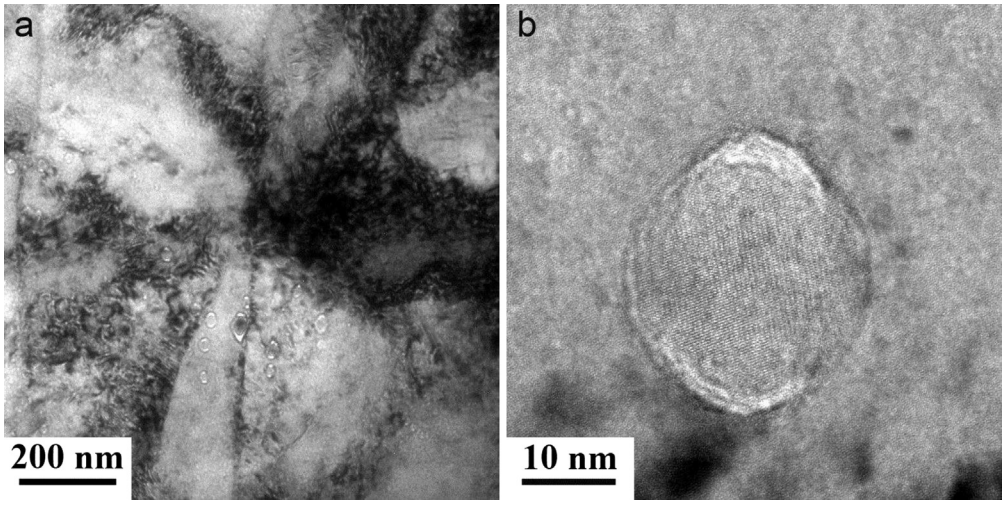

Fig. 3. TEM micrographs of hydrogen pre-charged (93 appm) ODS-EUROFER steel after CERT testing at strain rate of 10^{-4} s^{-1}: (a) general view; (b) HRTEM image of yttrium oxide particle.

Mechanical loading under specified conditions (2 kN, strain rate of 10^{-4} s^{-1}) did not affect the mean density and the size distribu tion of yttrium oxide particles. Importantly, no additional irregu larities or distortion on the oxide matrix interface were induced by the tensile test (Fig. 2b). At the same time, the loading increases the dislocation density significantly (Fig. 2a).

The microstructure of hydrogen charged ODS EUROFER steel after tensile testing is shown in Fig. 3. The combined action of hy drogenation and mechanical loading does not lead to any notice able change in either the density or size distribution of oxide nanoparticles. However, in contrast to as supplied samples, the interfaces of yttrium oxide particles with the ferrite matrix are distorted notably, becoming elongated in the tensile loading di rection (Fig. 3b). The observed structural irregularities can reach up to 10 nm in length depending on the nanoparticle size. This kind of distortion was observed around almost all nanoparticles located over the entire range of investigated depths from the steel surface (from 20 nm to 7 μm).

In order to understand the structure of the strain induced distortion around the ODS nanoparticles in hydrogen charged samples, the EDX analysis was carried out along the distorted particle (Fig. 4). In contrast to the EDX spectra for as supplied samples [17], that for distorted particle reveals a discontinuity of elemental content (Fig. 4b). Specifically, the EDX scan across the distorted particle matrix interface, as shown in Fig. 4a, shows that the point where the concentration of the matrix element (iron) starts to decrease (x~17 nm at the left, and x~78 nm at the right, Fig. 4b) is different from that where the concentration of ODS particle elements starts to increase (x~28 nm at the left and x~72 nm at the right, Fig. 4b). This gap reaches 6–11 nm. That is notably larger than the thickness 1–1.5 nm of the oxide shell [17].

This distribution of the elemental content indicates that the detected structural irregularity in the region of the matrix/particle interface is an open space between the oxide particle and the matrix. This means that hydrogen accumulation induces a loss of cohesion at the interface between the yttrium oxide nanoparticle and the matrix when the ODS EUROFER steel is subjected to tensile loading. It should be also noted, according to the EDX intensity profile of Cr in Fig. 4b, that the de cohesion of the particles occurs in such a way that Cr rich shell region (located at x~12 nm and x~85 nm in Fig. 4b) separates from the particle and remains at the matrix side.

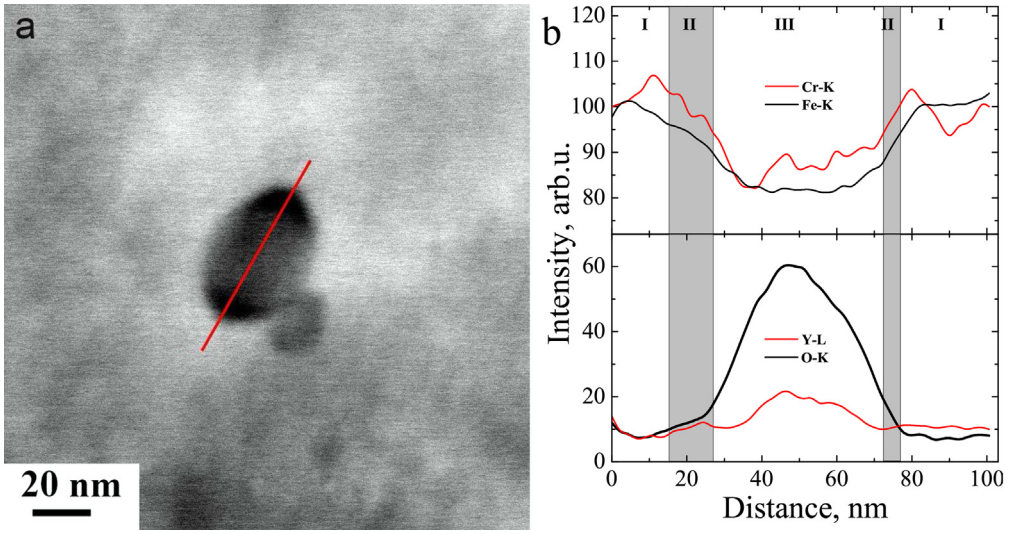

Fig. 4. (a) STEM micrograph of a distorted oxide particle (red line is area of EDX measurement); (b) the intensity profiles of EDX line scans: I matrix, II distorted zone, III oxide particle. (For interpretation of the references to colour in this figure legend, the reader is referred to the web version of this article.)

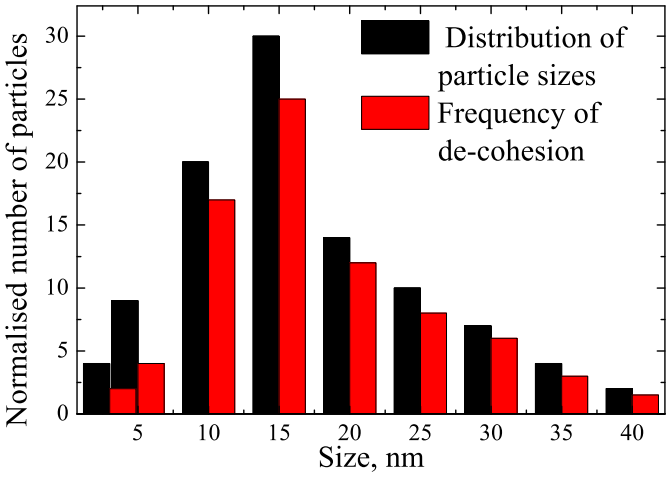

Fig. 5. Nanoparticle size distribution: total and those experienced de-cohesion.

Statistically (Fig. 5), 85% of ODS nanoparticles larger than 5 nm manifest hydrogen enhanced de cohesion at the nanoparticle/matrix interface, independent of the size of the nanoparticle. In contrast, only 40% of nanoparticles with the size less than 5 nm experienced de cohesion.

The reduction in the de cohesion frequency may be related to a higher degree of the interface coherence of the smaller nano particles, which makes the interface less attractive for hydrogen accumulation.

3.3. *First principles molecular dynamicssimulations*

The analysis of microstructural evolution in ODS EUROFER steel and the TDS measurements during mechanical tensile testing show that under the same mechanical loading only hydrogen pre charged samples demonstrate the loss of cohesion between yttrium oxide nanoparticles and ferrite matrix. It seems reasonable to assume that hydrogen trapping at the interface promotes interface weakening, which affects the interface cohesion violation under the action of external loading. On the other hand, there is no unanimous opinion in the literature on the efficiency of H trapping at the oxide steel interface, either confirming [18] or rejecting it [19].

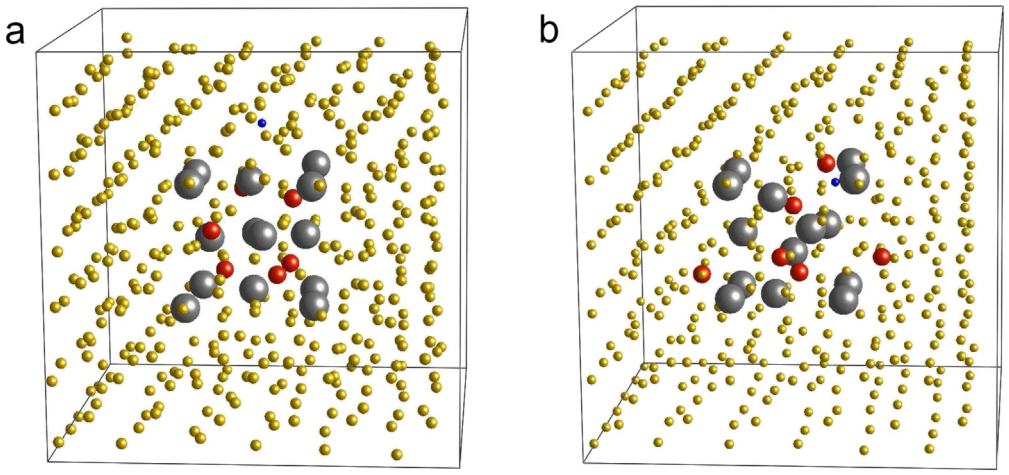

Fig. 6. Simulation cell (a) at the start and (b) at the end of MD simulation. The yellow spheres denote iron atoms, blue spheres are hydrogen atoms, gray and red spheres are yttrium and oxygen atoms, respectively. (For interpretation of the references to colour in this figure legend, the reader is referred to the web version of this article.)

First principles MD simulations of hydrogen atom behavior near a small yttrium oxide cluster embedded in bcc iron matrix performed in this study are in favor of hydrogen trapping at the oxide matrix interface. In these simulations, a hydrogen atom was positioned inside the iron matrix at a small distance from the particle surface (see Fig. 6a) and its dynamics was studied by MD as described in sect. 2. In spite of a short overall simulation time (140 fs), it was sufficient for the H atom to move quickly towards the oxide cluster surface and become trapped at an oxygen atom that shifted closer towards the interface. The O–H pair moved in a synchronous way, indicating the formation of a hydroxide (OH) group. Interestingly, the shift of the oxygen atom from the equilibrium position in the cluster interior towards the surface was not due to the effect of H atom; in fact, three oxygen atoms drifted eventually into octahedral positions in the particle matrix interface at the end of the simulation (see Fig. 6b). This is possibly an indication that the interface should be preferably decorated with oxygen atoms rather than with yttrium ones.

4. Conclusions

The presence of yttrium oxide particles in ODS EUROFER steel leads to a notable (by a factor of 5) increase in its hydrogen uptake as compared to ODS free EUROFER 97 steel. Microstructural TEM study suggests that hydrogen promotes de cohesion at the oxide particle/matrix interface under the action of mechanical loading. The modeling of hydrogen atom behavior at the oxide/matrix interface indicates that the interface weakening can be due to the hydrogen trapping with the formation of OH groups at the interface.

Acknowledgment

Authors acknowledge Dr. I. Golovchanskiy and Dr. P. Dzhumaev for fruitful discussions. Authors also wish to thank the Center for Scientific Computing (Helsinki, Finland) and the CSC Helios Supercomputer (Rokkasho, Japan) for the use of their computational facilities.

References

[1] R. Lindau, A. Moeslang, M. Schirra, P. Schlossmacher, M. Klimenkov, J. Nucl. Mater 307–311 (2002) 769–772.
[2] L. Hsiung, M. Fluss, S. Tumey, J. Nucl. Mater 409 (2011), 72–29.
[3] R. Lindau, A. Moeslang, M. Rieth, M. Klimiankou, Fusion Eng. Des. 75–79 (2005) 989–996.
[4] K. Yutani, H. Kishimoto, R. Kasada, J. Nucl. Mater 367–370 (2007), 432–427.
[5] A. Ryazanov, O. Chugunov, S. Ivanov, S. Latushkin, R. Lindau, A. Moeslang, A. Nikitina, K. Prikhodko, E. Semenov, V. Unezhev, P. Vladimirov, J. Nucl. Mater 442 (2013) 153–157.
[6] L. Fave, M.A. Pouchon, M. Dobeli, J. Nucl. Mater 445 (2014) 235–240.
[7] P. Vladimirov, A. Moeslang, J. Nucl. Mater 329–333 (2004) 233–237.
[8] T. Michler, M.P. Balogh, Int. J. Hydrogen Energy 35 (2010) 9746–9754.
[9] Y. Yagodzinskyy, E. Malitckii, M. Ganchenkova, S. Binyukova, O. Emelyanova, T. Saukkonen, H. Hanninen, R. Lindau, P. Vladimirov, A. Moeslang, J. Nucl. Mater 444 (2014) 435–440.
[10] T. Tanaka, K. Oka, S. Ohnuki, S. Yamashita, T. Suda, S. Watanabe, E. Wakai, J. Nucl. Mater 329–333 (2004) 294–298.
[11] G. Kresse, J. Furthmuller, Phys. Rev. B 54 (1996) 1169–1186.
[12] J. Perdew, K. Burke, M. Ernzerhof, Phys. Rev. Lett. 77 (1996) 3865–3868.
[13] I. Maroef, D.L. Olson, M. Eberhart, G.R. Edwards, Int. Mater. Rev. 47 (2002) 191–223.
[14] F.G. Wei, K. Tsuzaki, Gaseous Hydrogen Embrittlement of Materials in Energy Technologies, Woodhead Publishing in Materials, Oxford, 2012, pp. 493–525.
[15] W. Choo, J. Lee, Metall. Trans. A 13A (1982) 135–140.
[16] E. Malitckii, Y. Yagodzinskyy, M. Ganchenkova, S. Binyukova, H. Hanninen, R. Lindau, P. Vladimirov, A. Moeslang, Fusion Eng. Des. 88 (2013) 2607–2610.
[17] M. Klimenkov, R. Lindau, A. Moeslang, J. Nucl. Mater 386–388 (2009) 553–556.
[18] G. Esteban, A. Pena, F. Legarda, R. Lindau, Fusion Eng. Des. 82 (2007) 2634–2640.
[19] V. Sagaradze, V. Shalaev, V. Arbuzov, B. Goshchitskii, Y. Tian, W. Qun, S. Jiguang, J. Nucl. Mater 295 (2001) 265–272.